4th International Conference on Earthquake Engineering
Taipei, Taiwan
October 12-13, 2006

Paper No. 152

WEAKENED AND STRENGTHENED STEEL MOMENT CONNECTIONS

Chung-Che Chou[1], Chia-Ching Wu[2], Chih-Kai Jao[2], and Yuang-Yu Wang[3]

ABSTRACT

The effectiveness of using reduced flange plates (RFPs) or rib plates for seismic response of steel moment connections was investigated through cyclic testing of six full-scale specimens. The first scheme utilized RFPs to connect the beam flanges to the column, without any direct connection of the beam flange to the column. Plastic hinges were forced to form in the RFPs instead of the steel beam due to strong beam-weak RFPs, so the weakened moment connection eliminated buckling of the beam and reduced cost of repairing after earthquakes. The second scheme was to strengthen a connection, which was removed from an existing 33-story steel building, by welding rib plates between the column face and inner side of the beam flanges. Test results of the weakened connections showed that (1) the connections developed beam plastic moment and reach more than an interstory drift of 4% without strength degradation, (2) the RFP was effective in dissipating energy before buckling, and (3) no buckling of the beam was observed. Test results of the strengthened connection showed that the rib plates significantly reduced the beam flange strain by 75% compared to a non-retrofitted steel moment connection. Both types of connection specimens were modeled using the non-linear finite element computer program ABAQUS to perform a correlation study.

Keywords: Moment Connection, Cyclic Test, RFP, Rib Plate, Finite Element Analysis

INTRODUCTION

Since the 1994 Northridge earthquake, a lot of research has been performed to identify better moment connections for new steel moment frames and to improve poor moment connections for existing steel moment frames. These connection details, such as introducing a flat plate outside the beam flange (Whittaker et al. 2001, Kim et al. 2002, Engelhardt and Sabol 2002) or reduced section in the beam flange (Engelhardt et al .1996, Chen et al. 1996, Uang et al. 2000), are intended to force inelastic deformation of the beam away from the column face. This paper presents data from experiments conducted by the writers on six specimens using weakened and strengthened moment connections. Instead of using the reduced beam section to weaken the beam flexural capacity, four weakened moment connections use Reduced Flange Plates (RFPs) to connect the steel beam flange and the column; no direct connection between the beam flange and the column. A circular reduced section, designed based on the concept of strong beam-weak RFPs, is introduced in the flange plates to limit inelastic deformation in the plate not the beam. The connections achieve cyclic performance similar to the flange plate moment connection but prevent steel beams from buckling. Two moment connections, removed from an existing steel frame, have pre-Northridge connection details, which violate requirements by FEMA 350 (2000). To minimize amount of work for retrofitting the building, one of the specimens uses rib plates between the column and inner side of the beam flanges to strengthen the connection. Ideally, the strain in the beam flange near the column would be reduced and buckling of the beam would be forced away from the column.

[1]Assist. Professor, Dept. of Civil Engineering, National Chiao Tung University, Hsinchu, Taiwan, chchou@mail.nctu.edu.tw
[2]Graduate Student Researcher, Dept. of Civil Engineering, National Chiao Tung University, Hsinchu, Taiwan
[3]President, Spring Tech Consultants, Inc., Taipei, Taiwan

TWO TYPES OF PROPOSED MOMENT CONNECTIONS

Weakened Moment Connection

Four new weakened moment connection subassemblies (Chou et al. 2005) were designed and tested. Each subassembly included an exterior connection with one steel beam (H450×200×9×14) and a concrete-filled tube column (350×350×9). ASTM Grade 50 steel was specified for the beam and tube column. As shown in Fig. 1, the connection used the reduced flange plate (RFP) to transfer the beam flange force to the column. The ultimate flexural capacity, M_{RFP}, provided by the RFPs is estimated as

$$M_{RFP} = F_u \; b_R \; t_R \; \left(d_b + t_R\right) \tag{1}$$

where b_R is the minimum width of the RFP; t_R is the thickness of the RFP; d_b is the beam depth, and F_u is the specified ultimate tensile strength of the plate, equal to 400 MPa and 450 MPa for ASTM A36 and Grade 50 material, respectively. The moment at the column face, determined by projecting the moment capacity, M_{RFP}, at the center of the reduced section, is

$$M_{RFPF} = F_u b_R t_R \left(d_b + t_R\right) \frac{L_b}{L_b - s_h} \tag{2}$$

where s_h is the distance between the face of the column and the center of the reduced section, and L_b is the distance from the actuator to the face of the column. When the beam yield moment, M_{yb}, is developed at the end of the RFP, the moment at the face of the column is

$$M_{yf} = M_{yb} \frac{L_b}{L_b - \left(L_{RFP} + d_b/4\right)} \tag{3}$$

where L_{RFP} is the length of the RFP, and $d_b/4$ is the distance between the beam hinge and the end of the RFP.

Since all specimens were intended to produce plastic hinges in the RFPs, the size of the RFPs was determined by limiting M_{RFPF} less than either M_{yf} (Specimens RFP-1, RFP-2, and RFP-3) or $0.9M_{yf}$ (Specimen RFP-4). The minimum width of the RFP, b_R, for all specimens was 120 mm. ASTM Grade 50 steel was used for the RFPs of Specimens RFP-1 and RFP-2, and ASTM A36 steel was used for the RFPs of Specimens RFP-3 and RFP-4. The thickness, t_R, flexural capacity, M_{RFP}, and the computed moment from Eqs. (2) and (3) are listed in Table 1. The RFPs of Specimens RFP-1 and RFP-2 were shop welded to the column tube since shop fabrication can produce high quality welds. Specimen RFP-1 used a bearing-type joint between the RFP and the beam flange, in which bolt shear controlled the number of bolts. The design force for the bolts was computed as the moment, M_{RFP}, divided by the distance between mid thickness of the top and bottom RFPs. Specimen RFP-2 used pretensioned slip-critical high-strength bolts along with longitudinal fillet welds to connect the RFP and the beam flange (Fig. 2). Two stiffeners outside the RFPs were intended to reduce the buckling length of the RFP. Specimens RFP-3 and RFP-4 used a device, which is composed of the RFP and an end plate, to connect the column and the beam. The device of Specimen RFP-3 was shop welded outside the beam flange and field bolted to the column with A490 bolts. Specimen RFP-4 used bearing-type bolts to connect the device and the beam flange, and also had a T-shaped stiffener outside the RFP to prevent buckling of the RFP in compression.

Strengthened Moment Connection

Two moment connections RMC-1 and RMC-2 were removed from an existing moment frames and delivered to the laboratory for testing (Chou et al. 2006). Weld backing and runoff tabs were left in the CJP groove welds between the beam and column; a circular-cut weld access hole with radius of 50 mm was used; and the shear tab was bolted to the beam web reinforced with fillet welds. These connection details violate requirements for use in Special Moment Frame systems by FEMA-350 (2000). Complete joint penetration (CJP) groove welds of these two specimens were also examined by ultrasonic test; the results showed that CJP groove weld of Specimen RMC-1 was acceptable but that of Specimen RMC-2 had defect. To minimize the amount of work required to retrofit the existing moment frame, welding four 22-mm thick rib plates (Fig. 3) between the box column (700×700×35)

and the inner side of the beam (H702×254×16×28) flanges was proposed. Ideally, the beam flange strain in the strengthened section would be reduced by more than half compared to the non-retrofitted moment connection.

TEST RESULTS

Weakened Moment Connection

Each specimen was tested in the setup (Fig. 4) by displacing an actuator at the end of the beam through a series of displacement cycles (AISC 2002). Fig. 5 shows the relationships between the beam tip deflection and the moment for Specimens RFP-1 and RFP-2. The cyclic behavior shows that, in general, the reduced flange plate absorbed a significant amount of inelastic energy although the inelastic behavior of Specimen RFP-1, same as Specimen RFP-4, was pinched due to slip of the bolted RFP joint. At an interstory drift of 0.75%, the flange force of Specimens RFP-1 and RFP-4 reached the friction slip capacity of the bolts, and the beam flange slipped, causing an increase in drift under almost constant moment ($0.61M_{np}$). Further application of the load caused bolts to bear against the bolt holes, and considerable stiffness gained after an interstory drift of 1.5%. The maximum moment of Specimen RFP-1 was developed at an interstory drift of 5%, where buckling of the RFP in compression was noticed. The buckled RFP could be straight in tension but the flexural strength degraded at an interstory drift of 6% due to buckling of the RFP (Fig. 6). With a T-shaped stiffener positioned outside the RFP of Specimen RFP-4, buckling of the RFP was not noticed until the specimen was loaded towards an interstory drift of 7%.

A fully-restrained joint was used to connect the RFPs and the beam flanges for Specimens RFP-2 and RFP-3. The RFP yielded at an interstory drift of 1% when the moment at the column face reached $0.8M_{np}$. Buckling of the RFP became apparent at an interstory drift of 4% for both specimens. Fracture of the top RFP in tension, as illustrated by Fig. 7, occurred at the second cycle of 5% interstory drift that was imposed on Specimen RFP-2. Welding between the buckled RFP and the beam flange of Specimen RFP-3 fractured at an interstory drift of 4%; the fracture propagated with an increasing drift and caused a sudden loss in strength towards a 6% interstory drift.

Strengthened Moment Connection

Specimen RMC-1 remained elastic through all cycles of 0.375%, 0.5%, and 0.75% interstory drift. Yielding of CJP groove weld near the weld tab, as indicated by the flaking of whitewash, began at an interstory drift of 1%. Yielding was also observed at a weld access hole and at a junction of the shear tab to the column at an interstory drift of 1.5%. A minor weld crack was observed at the beam top flange near the weld tab and at the toe of the shear tab to the column face at the first cycle of 3% interstory drift. A minor crack was also observed at the end of the weld access hole near the beam flange. No strength degradation was observed during the excursion of 3% interstory drift [Fig. 8(a)], so the test was continued to the first cycle of 4% interstory drift when fracture of the beam flange occurred suddenly [Fig. 9(a)].

Specimen RMC-2 retrofitted with rib plates experienced similar behavior as Specimen RMC-1 before an interstory drift of 2%, but no sign of yielding was observed at a weld access hole or at the junction of the shear tab to the column. A minor weld crack within the weld tab length was observed at an interstory drift of 2%, and the crack propagated along the CJP groove weld at the first cycle of a 3% drift. A complete weld fracture along the beam top flange and welded rib plates occurred at the second cycle of 3% interstory drift [Fig. 9(b)], resulting in significant strength degradation [Fig. 8(b)]. Since the CJP groove weld at the beam bottom flange showed no sign of crack, the test was loaded reversely to an interstory drift of -4.8%. A minor weld crack near the toe of the rib plate and the column was observed, but no CJP weld fracture was observed at the beam bottom flange and column. Strain gages in the beam flange 60 mm away from the column face showed that the rib plates significantly reduce the tensile strain from 4% to 1% compared to Specimen RMC-1 and RMC-2 (Fig. 10). Note that the significant strain reduction cannot prevent fracture of the CJP groove weld due to existing weld defect in Specimen RMC-2 not Specimen RMC-1.

FINITE ELEMENT ANALYSIS

Finite element analysis was undertaken to study the flexural behavior between the proposed connection (Specimen RFP-2) and the flange plate (FP) moment connection, which is a prequalified moment connection according to FEMA-350 (2000). A FP connection with 16-mm thick flange plates outside the beam flange was determined based on FEMA-350 (2000). The two connections were modeled with the computer program ABAQUS (2003). The steel beam, steel tube, flange plate, and RFP were modeled using four-node shell elements, S4R. Rigid links were incorporated to simulate welding between the beam flange and the RFP or flange plate; they were also used to model the bolted connection between the beam flange and the RFP and between the beam web and the shear tab. Since the CFT column remained elastic during the test, the concrete infill were modeled as having only elastic properties. Eight-node solid elements, C3D8R, were used with contact modeling between the steel and concrete. Interaction between the concrete and the steel tube was modeled with hard contact behavior, allowing separation of the interface in tension and no penetration of that in compression. Steel coupons were tested cyclically in order to determine suitable parameters (Chou et al. 2005) in predicting the hysteretic behavior of the steel using the combined isotropic and kinematic hardening model in the computer program ABAQUS.

The moment versus beam tip deflection relationship of Specimen RFP-2 model is shown in Fig. 11(a); this relation predicts well the curves of cyclic test data. Fig. 12(a) shows longitudinal stress contour of the connection at the first cycle of an interstory drift of 4%, where the stress in the RFP concentrates within the reduced section. The steel beam of the FP connection buckles at the second cycle of an interstory drift of 4% [Fig. 12(b)]. The moment-deflection relationship of the FP connection is similar to that of Specimen RFP-2 before an interstory drift of 4% [Fig. 11(b)]. The elastic flexural stiffness and ultimate strength of the FP connection is 4% and 11% larger than that of Specimen RFP-2 model, indicating that flexural rigidity and strength of the proposed connection is close to the moment connection.

Nonlinear finite element analysis was performed and the analytical results were correlated with the experimental data for Specimens RMC-1 and RMC-2. Eight-node solid elements, C3D8R, were used to model the steel box column, steel beam, and rib plates. Rigid links were incorporated to simulate bolted joint between the beam web and the shear tab. The beam tip was loaded monotonically by imposing a displacement up to 3% interstory drift. Fig. 8 shows that the analytically predicted curve correlated closely the peak response of the test data for both specimens. The finite element analysis confirmed that the presence of the rib plate reduced the tensile strain in the beam flange of Specimen RMC-2 (Fig. 10) by more than 60%. Fig. 13 shows flexural stress and strain contours in the rib plates, indicating that only part of the rib plate was effective to transfer the beam flange force to the column and the size of the rib plate might be further reduced. By integrating flexural stresses along the rib plate and the beam flange near the column face, it was found that the tensile force carried by the rib plates is about 23% of that carried by the beam flange at an interstory drift of 3%.

CONCLUSIONS

Four weakened moment connections were tested and analyzed. Specimens RFP-1 and RFP-4 with the bearing-type joint between the RFP and the beam flange exhibited bolt slip at small drift, causing an increase in drift under almost constant moment until the bolts bore against the bolt holes. Specimens RFP-2 and RFP-3 used a weld joint between the RFP and the beam flange. Specimen RFP-3 experienced gradual weld fracture due to buckling of the RFP. Specimen RMC series were removed from an existing steel moment frame; Specimen RMC-2 had defect in CJP groove welds and was strengthened with four rib plates. Specimen RMC-1 and RMC-2 experienced fracture of the beam flange and CJP groove welds, respectively, at an interstory drift of 3%, violating AISC (2002) seismic provisions. Nonlinear finite element analyses of weakened and strengthened moment connections were performed using solid and shell elements. The experimental and analytical results support the following conclusions:

(1) Weakened moment connection reached beyond an interstory drift of 4% without yielding in the beam or significant strength degradation. The moment computed at the column face was about 1.2 to 1.34 times the nominal moment capacity of the beam (Fig. 5) at an interstory drift of 4%.
(2) The finite element analyses demonstrated that the proposed weakened connection and the flange plate connection exhibit a similar hysteretic behavior [Fig. 11(b)]. The elastic flexural stiffness of Specimen RFP-2 is about 4% lower than that of the flange plate connection, indicating that the flexural rigidity of the weakened connection is compatible to the moment connection.
(3) Specimen RMC-1 and RMC-2 had pre-Northridge connection details, violating requirements by FEMA 350 (2000). Although CJP groove welds of Specimen RMC-1, examined by ultrasonic test, were acceptable, the beam flange fractured at an interstory drift of 3%. The maximum tensile strain in the beam flange of Specimen RMC-2, which was strengthened with four rib plates (Fig. 3), was 1%, much less than 4% measured in Specimen RMC-1 at an interstory drift of 3% (Fig. 10).

ACKNOWLEDGMENTS

The researches sponsored by the National Center for Research on Earthquake Engineering (NCREE) and Spring Tech Consultants Inc., Taiwan are appreciated. The writers would also express gratitude to Professor K. C. Tsai for providing technical advices.

REFERENCES

AISC (2002). *Seismic provisions for structural steel buildings*. AISC, Chicago.

Chen, S. J., C. H. Yeh, and J. M. Chu (1996). "Ductile steel beam-to-column connections for seismic resistance," *J. Structural Engineering*, ASCE, Vol. 122, No. 11, 1292-1299.

Chou, C. C., C. C. Wu, and C. H. Chou (2005). Seismic behavior of steel reduced flange plate moment connections. *Report No. NCREE-05-017*, National Center for Research on Earthquake Engineering, Taipei, Taiwan (in Chinese).

Chou, C. C., Y. J. Lai, Y. C. Wang, C. P. Hsu (2006). Cyclic testing of retrofitted moment connections for a Kaohsiung existing steel building structure. Dept. of Civil Engineering, National Chiao Tung University, Hsinchu, Taiwan (in Chinese).

Engelhardt, M. D., T. Winneberger, A. J. Zekany, and T. Potyraj (1996). "The dogbone connection: Part II," *Modern Steel Construction*, AISC.

Engelhardt, M. D., and T. A. Sabol (2002). "Reinforcing of steel moment connections with cover pates: benefits and limitations," *Engineering Structures*, Vol. 20, No. 4-6, 510-520.

FEMA (2000). Recommended Seismic Design Criteria for New Steel Moment-Frame Building*s*, *FEMA 350*, Federal Emergency Management Agency, Washington, DC.

HKS (2003). *ABAQUS User's Manual Version 6.3*, Hibbitt, Karlsson & Sorensen, Inc., Pawtucket, RI.

Kim, T., A. S. Whittaker, A. S. J. Gilani, V. V. Bertero, and S. M. Takhirov (2002). "Experimental evaluation of plate-reinforced steel moment-resisting connections," *J. Structural Engineering*, ASCE, Vol. 128, No. 4, 483-491.

Schneider, S., and l. Teeraparbwong (2002). "Inelastic behavior of bolted flange plate connections," *J. Structural Engineering*, ASCE, Vol. 128, No. 4, 492-500.

Uang, C. M., Q-S Yu, S. Noel, and J. Gross (2000). "Cyclic testing of steel moment connections rehabilitated with RBS or Welded Haunch," *J. Structural Engineering*, ASCE, Vol. 126 (1), 57-68.

Whittaker, A. S., A. S. J. Gilani, S. M. Takhirov, and C. Ostertag (2002). "Forensic studies of a large cover-plate steel moment-resisting connection," *The Structural Design of Tall Buildings,* Vol. 7, 265-283.

Table 1. Parameters for Specimens RFP series

Specimen No.	t_R (mm)	M_{RFP} (kN-m)	M_{RFPF} (kN-m)	M_{RFPF}/M_{np}	M_{RFPF}/M_{yf}
RFP-1	22	561	620	1.11	0.93
RFP-2	22	561	620	1.11	0.93
RFP-3	25	570	627	1.12	0.93
RFP-4	20	508	557	1.00	0.83

Note: M_{np} is the nominal capacity of the beam

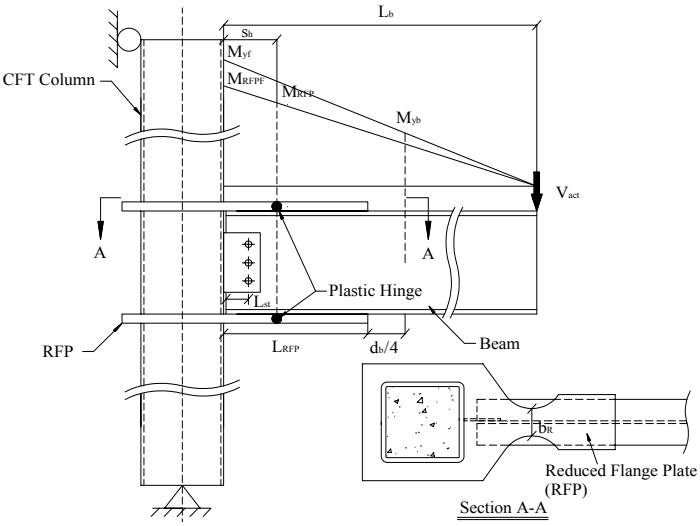

Figure 1. Moment distribution along beam length.

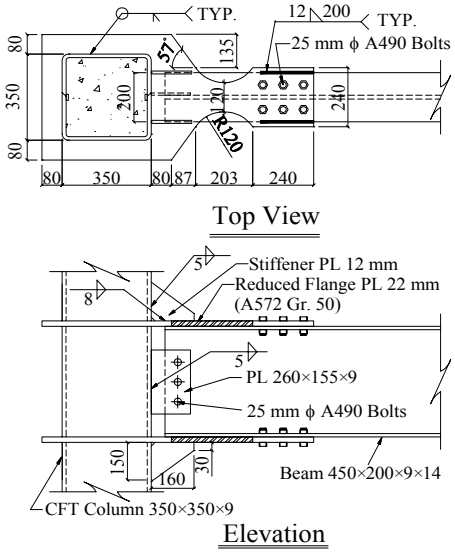

Figure 2. Specimen RFP-2 connection details.

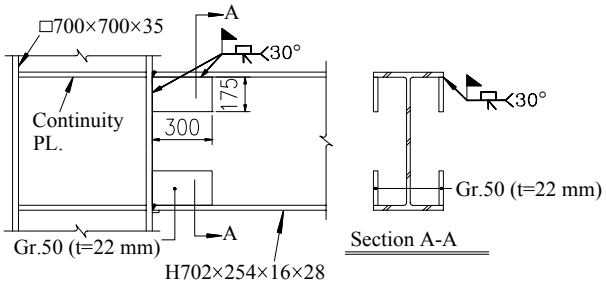

Figure 3. Specimen RMC-2 connection details.

Figure 4. Test setup.

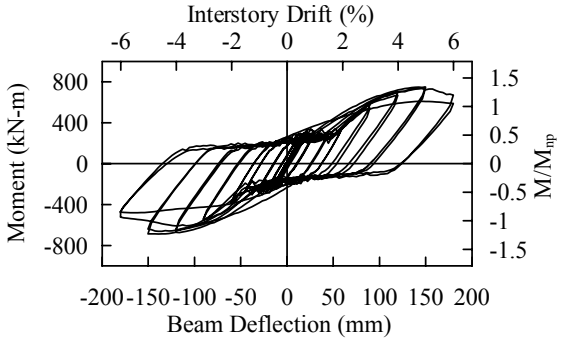

(a) Specimen RFP-1

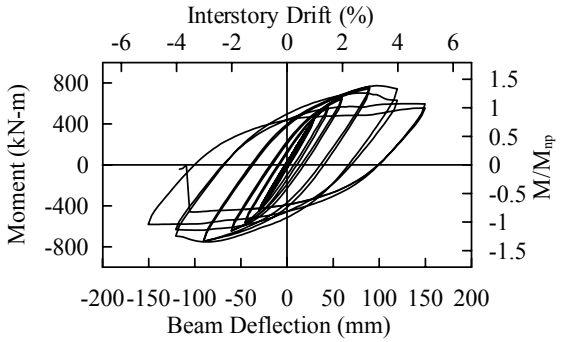

(b) Specimen RFP-2

Figure 5. Moment versus beam deflection relationship (weakened moment connections).

Figure 6. RFP buckling (Specimen RFP-1).

Figure 7. RFP fracture (Specimen RFP-2).

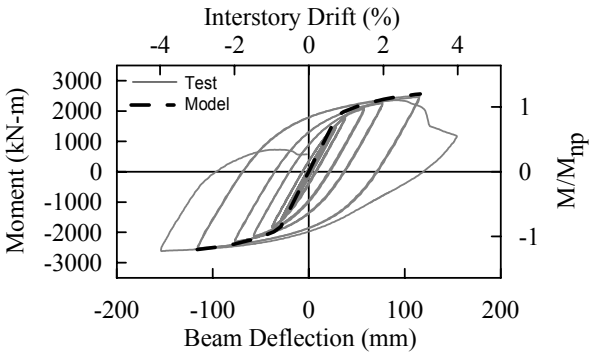

(a) Specimen RMC-1

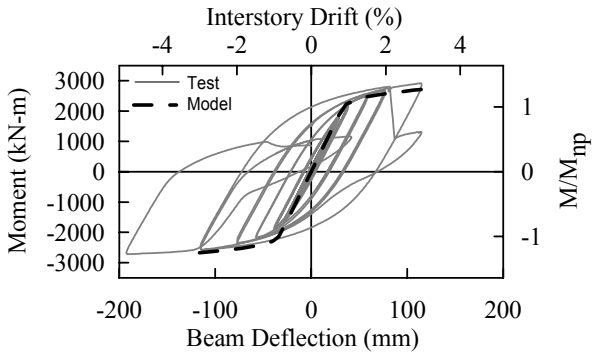

(b) Specimen RMC-2

Figure 8. Moment versus beam deflection relationship (strengthened moment connections).

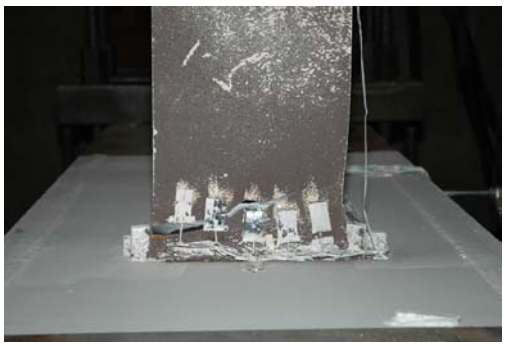

(a) Specimen RMC-1

(b) Specimen RMC-2

Figure 9. Failure of strengthened moment connections.

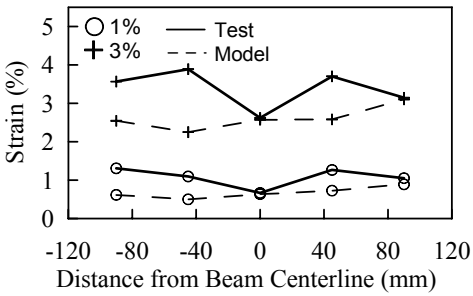

(a) Specimen RMC-1

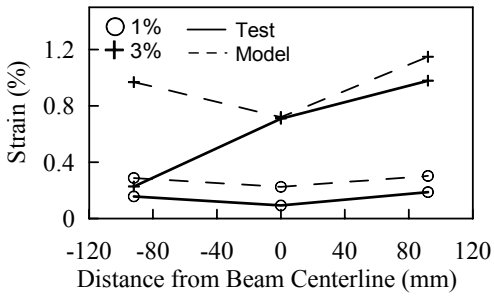

(b) Specimen RMC-2

Figure 10. Strain along the beam flange.

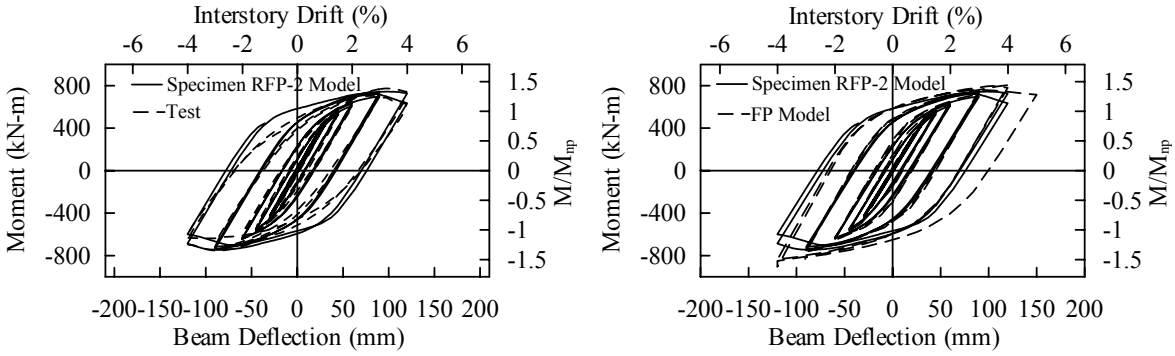

(a) Specimen RFP-2 model versus test result (b) Specimen RFP-2 model versus FP model

Figure 11. Moment versus beam deflection relationship between test and finite element model.

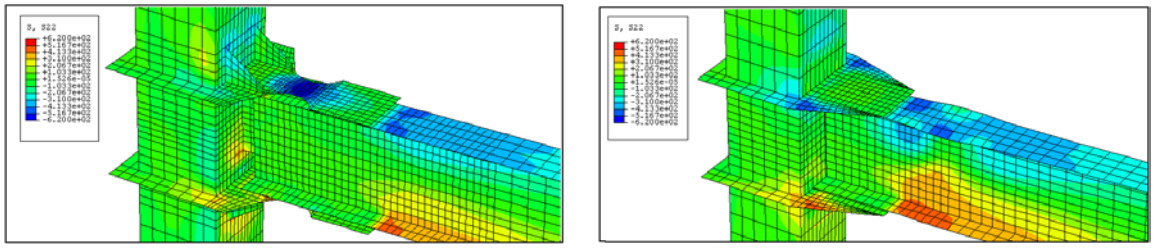

(a) Specimen RFP-2 model (b) FP model

Figure 12. Flexural stress contours of finite element models.

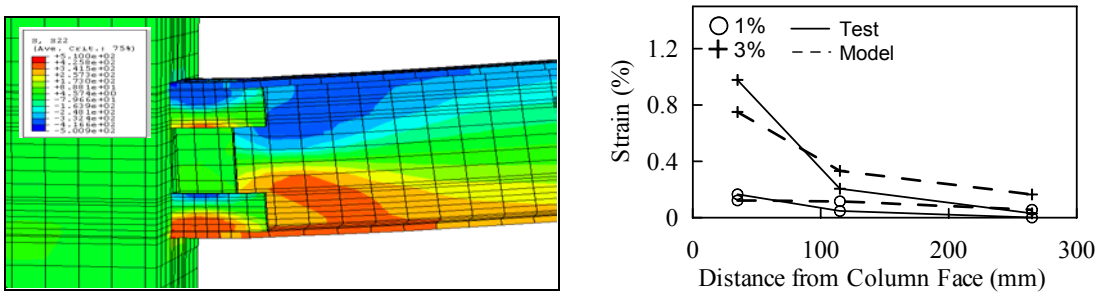

(a) Stress Contour (3% Drift) (b) Rib Strain Contours

Figure 13. Finite element model of Specimen RMC-2.